Current Journal of Applied Science and Technology

34(2): 1-14, 2019; Article no.CJAST.26905
ISSN: 2457-1024
(Past name: British Journal of Applied Science & Technology, Past ISSN: 2231-0843, NLM ID: 101664541)

Similarity Solution of Flow, Heat and Mass Transfer of a Nanofluid Over a Porous Plate in a Darcy-Forchheimer Flow

A. Falana[1] and A. Alao Ahmed[1*]

[1]Department of Mechanical Engineering, University of Ibadan, Ibadan, Nigeria.

Authors' contributions

This work was carried out in collaboration between both authors. Both authors read and approved the final manuscript.

Article Information

DOI: 10.9734/CJAST/2019/v34i230123
Editor(s):
(1) Dr. Luigi Maxmilian Caligiuri, Professor, Faculty of Science, University of Calabria, Italy and Foundation of Physics Research Center (Director)- FoPRC, Italy.
Reviewers:
(1) R. Ellahi, International Islamic University Islamabad, Pakistan.
(2) Zhi Shang, Institute of High Performance Computing, Singapore.
(3) Dr. R. Praveen Sam, G. Pulla Reddy Engineering College, Jawaharlal Nehru Technological University Anantapur, India.
Complete Peer review History: http://www.sdiarticle3.com/review-history/26905

Original Research Article

Received 20 May 2016
Accepted 01 August 2016
Published 30 March 2019

ABSTRACT

In this work, a similarity solution of the flow, heat and mass transfer of a nanofluid over a porous plate in a Darcy-Forchheimer flow is explored. The nanofluid model includes Brownian motion and Thermophoresis diffusion effects. The governing transport equations are made dimensionless using similarity transformation technique which reduce them into ordinary differential equations with the associated boundary conditions. The equations are then solved numerically using the classical fourth order Runge-Kutta method and the results are benched marked with available results in literature and are found to be in good agreement. The results for the flow velocity, the shear stress, the temperature distribution, the nanoparticle volume concentration, the skin friction coefficient, $f''(0)$, the reduced Nusselt number, $-\theta'(0)$ and the reduced Sherwood number, $-\phi'(0)$ are presented graphically illustrating the effects of permeability, inertia, thermophoresis, Brownian motion, Lewis number and Prandtl number on the flow. Our analysis shows, among others, that the Nusselt number is a decreasing function, while the Sherwood number is an increasing function of the thermophoretic number N_t.

**Corresponding author: E-mail: ahmadalao@gmail.com;*

Keywords: Brownian motion; Darcy-Forchheimer flow; nanofluid; thermophoresis; Runge-Kutta.

1. INTRODUCTION

Nanofluids have enormous potentials in enhancing heat transfer performances because of their thermo-physical properties when compared to their base fluids or conventional particle fluid suspensions. They are used as coolants in microchip computers, advanced nuclear systems, microfluidic electronics, fuel cells, biological sensors, hybrid power engines etc. Carbon nanotubes and diamond nanoparticles have also found important applications in nanotechnology. Choi [1] first introduce a nanotechnology concept which uses a mixture of nanoparticles and the base fluid in order to develop advanced heat transfer fluids with substantially higher conductivities. Nanoparticles are made of oxides such as carbides, silica, alumina, copper oxides etc. Buongiorno [2] made a comprehensive survey of convective transport in nanofluids. He explained the enhanced heat transfer characteristics of nanofluids and their abnormal increase in thermal conductivities as a result of two main effects, namely, the Brownian diffusion and the thermophoretic diffusion of the nanoparticles. Ellahi et al. [3] studied *S*hape effects of nanosize particles in Cu-H_20 nanofluid on entropy generation. Khan and Pop [4] used the model of Kuznetsov and Nield [5] to study the fundamental work on the boundary layer flow of nanofluid over a stretching sheet.

Very recently, Rahmat et al. [6] investigated the Simultaneous effects of nanoparticles and slip on Jeffrey fluid through tapered artery with mild stenosis. Moreover, Zeeshan et al. [7] studied the Effect of magnetic dipole on viscous Ferro-fluid past a stretching surface with thermal radiation. Mohsen and Rahmat [8] studied Electro hydrodynamic nanofluid hydrothermal treatment in an enclosure with sinusoidal upper wall. Sheikholeslami et al. [9] discussed the effect of thermal radiation on nanofluid flow and heat transfer using two phase model. Ellahi et al. [10] studied problems on Natural convection MHD nanofluid by means of single and multi-walled carbon nanotubes suspended in a salt water solution. Kandelousi et al. [11] also studied the *S*imulation of Ferro fluid flow for magnetic drug targeting using Lattice Boltzmann method. Saman et al. [12] Study stream wise transverse magnetic fluid flow with heat transfer around a porous obstacle. Sher Akbar et al. [13] have studied the Influence of induced magnetic field and heat flux with the suspension of carbon nanotubes for the peristaltic flow in a permeable channel. Sheikholeslami and Ellahi [14] work on three dimensional mesoscopic simulation of magnetic field effect on natural convection of nanofluid.

It is important to note that Darcy's classical flow model is a fundamental law relating the pressure gradient, viscosity and fluid velocity linearly through porous medium. Any deviation from Darcy's law and assumptions is termed as non-Darcy flow. Darcy's law works for creeping fluids of Reynolds number (Re) within a range of 1 to 10 Ishak et al. [15]. Most often, it is assumed that the upper limit of the applicability of Darcy's law is between Re of (1 and 2) Bear [16]. Chen et al. [17] argued that the momentum equation most reduce to the viscous flow limit and advocate that frictional terms be added in Darcy's flow model for flow through a porous medium. The aim of this paper is to analyze flow, heat and mass transfer of a nanofluid over a porous plate using the Darcy-Forchheimer model.

However, to the best of author's knowledge, no attempt has been made to analyze flow, heat and mass transfer of a nanofluid over a porous plate in a Darcy-Forchheimer flow. Hence, the problem is investigated. The governing partial differential equations are transformed to a system of ordinary differential equations using similarity approach and the resulting equations are then solved numerically using the classical fourth order Runge-Kutta method. An investigation is carried out to illustrate the effect of various governing parameters viz., the velocity, shear stress, temperature, concentration, skin friction coefficient, Nusselt and Sherwood number are discussed in details.

2. FORMULATION OF THE PROBLEM

Consider a steady, two-dimensional, incompressible boundary layer flow of a nanofluid over a porous plate embedded in a porous medium. The x-axis is taking along the surface of the porous plate and the y-axis perpendicular to it. The temperature T_w and concentration C_w on the surface of the plate are kept constant, and assumed to be greater than the ambient temperature and concentration, T_∞ and C_∞, respectively. A physical geometry of the model is given in Fig. 1. In this analysis, the partial differential equation governing the

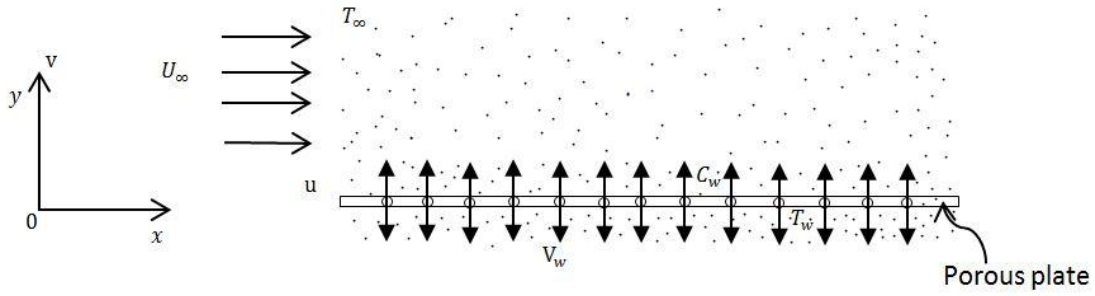

Fig. 1. Geometry of the physical model

Momentum fluid flow is based on Darcy-Forchheimer model which consist of linear and non-linear, Drag and Inertia, respectively. The governing equations of the flow field can be written in dimensional form as:

$$\frac{\partial u}{\partial x} + \frac{\partial \mathrm{v}}{\partial y} = 0. \tag{1}$$

$$u\frac{\partial u}{\partial x} + \mathrm{v}\frac{\partial u}{\partial y} = v\frac{\partial^2 u}{\partial y^2} - \frac{v}{\kappa}(u - u_\infty) - \frac{\kappa'}{\sqrt{\kappa}}(u^2 - u_\infty^2). \tag{2}$$

$$u\frac{\partial T}{\partial x} + \mathrm{v}\frac{\partial T}{\partial y} = \alpha\frac{\partial^2 T}{\partial y^2} + \tau[D_B\frac{\partial C}{\partial y}\left(\frac{\partial T}{\partial y}\right) + \frac{D_T}{T_\infty}\left(\frac{\partial T}{\partial y}\right)^2]. \tag{3}$$

$$u\frac{\partial C}{\partial x} + \mathrm{v}\frac{\partial C}{\partial y} = D_B\left(\frac{\partial^2 C}{\partial y^2}\right) + \frac{D_T}{T_\infty}\left(\frac{\partial^2 T}{\partial y^2}\right). \tag{4}$$

Where u and v are the velocity components in the x and y directions respectively, u_∞ is the free stream velocity, μ is the viscosity, T is the temperature of the nanofluid, C is the concentration of the nanofluid, T_w is the temperature along the porous plate, C_w is the concentration along the porous plate, T_∞ and C_∞ are the ambient temperature and concentration respectively, $v = \frac{\mu}{\rho}$ is the kinematic viscosity, $\kappa = \kappa_0 x$ is the Darcy permeability of the porous medium, κ_0 is the inertial permeability, $\kappa' = \frac{\kappa_0'}{\sqrt{x}}$ is the Forchheimer resistance, κ_0' is the Forchheimer constant, $\mathrm{D_B}$ is the Brownian motion coefficient, $\mathrm{D_T}$ is the thermophoresis coefficient, k is the thermal conductivity, $(\rho c)_p$ is the heat capacitance of the nanoparticles, $(\rho c)_f$ is the heat capacitance of the base fluid, $\alpha = \frac{k}{(\rho c)_f}$ is the thermal diffusivity, $\tau = \frac{(\rho c)_p}{(\rho c)_f}$ is the ratio between the heat capacitance of the nanoparticles and the heat capacitance of the base fluid.

With the associated boundary conditions

$$u = 0, \mathrm{v} = 0 \;\; T = T_w, C = C_w \; at \; y = 0 \tag{5a}$$

$$u \to u_\infty, T \to T_\infty, C \to C_\infty \; as \; y \to \infty \tag{5b}$$

With $u = \frac{\partial \psi}{\partial y}$ and $\mathrm{v} = -\frac{\partial \psi}{\partial x}$, the continuity equation in (1) is satisfied automatically, where $\psi(x, y)$ is the stream function.

The following dimensionless parameters are introduced in order to transform the governing equations into a set of ordinary differential equations:

$$\psi(x, y) = \sqrt{u_\infty v x} f(\eta),$$
$$\eta = \left({}^{y}/_{x}\right)(Re_x)^{\frac{1}{2}} = y\sqrt{\frac{u_\infty}{vx}},$$
$$\theta(\eta) = \left(\frac{\mathrm{T} - \mathrm{T}_\infty}{\mathrm{T_w} - \mathrm{T}_\infty}\right),$$
$$\phi(\eta) = \left(\frac{\mathrm{C} - \mathrm{C}_\infty}{\mathrm{C_w} - \mathrm{C}_\infty}\right). \tag{6}$$

In view of the above similarity variables, the equations (2)-(4) reduce to

$$f''' + \frac{1}{2} f f'' - \kappa_1(f' - 1) - \kappa_2\left[(f')^2 - 1\right] = 0. \tag{7}$$

$$\frac{\theta''}{Pr} + Nb\,\phi'\theta' + Nt\,(\theta')^2 + \frac{1}{2} f\,\theta' = 0. \tag{8}$$

$$\phi'' + \frac{Nt}{Nb}\theta'' + \frac{Le}{2} f\,\phi' = 0. \tag{9}$$

The transformed boundary conditions are:

$$f = 0\,, f' = 0, \theta = 1, \phi = 1 \,\mathrm{at}\, \eta = 0 \tag{10a}$$

$$f' \to 1, \theta \to 0, \phi \to 0 \text{ as } \eta \to \infty \quad (10b)$$

Where prime denotes first differential with respect to η and double prime denotes second differential etc. The parameters in equations (7-9) are defined as follows:

$$\kappa_1 = \frac{1}{Da_x Re_x} = \frac{\upsilon}{\kappa_o u_\infty}, Da_x = \frac{\kappa}{x^2} = \frac{\kappa_o}{x},$$
$$Re_x = \frac{u_\infty x}{\upsilon}, \kappa_2 = \frac{\kappa_o'}{\sqrt{\kappa_o}}, Pr = \frac{\nu}{\alpha},$$
$$Nb = \frac{\tau}{\nu} D_b (C_w - C_\infty),$$
$$Nt = \frac{\tau}{\nu}\frac{D_T}{T_\infty}(T_w - T_\infty), Le = \frac{\upsilon}{D_B}. \quad (11)$$

Where $\kappa_1, Da_x, Re_x, \kappa_2, P_r, N_b, N_t$ and L_e represents the permeability parameter of the porous medium, the local Darcy number, the local Reynolds number, the inertial parameter, the Prandtl number, the Brownian motion parameter, the thermophoresis parameter and the Lewis number respectively. Physical quantities of interest in this study are the local Nusselt number Nu_x, local Sherwood number Sh_x and the skin friction coefficient C_f which are defined as:

$$Nu_x = \frac{x q_w}{K(T_w - T_\infty)}, Sh_x = \frac{x q_m}{D_B(C_w - C_\infty)},$$
$$C_f = \frac{\tau_w}{\rho U_w^2}. \quad (12)$$

Where $\mathrm{k}, C_f, q_w,$ and q_m are the thermal conductivity, the wall skin friction, the surface heat flux and the wall mass flux respectively.

$$\tau_w = \mu \frac{\partial u}{\partial y}, q_w = -\mathrm{k}(\frac{\partial T}{\partial y})_{y=0},$$
$$q_m = -D_B(\frac{\partial C}{\partial y})_{y=0}. \quad (13)$$

Using (6) in (12), we can obtain the dimensionless skin friction coefficient, Nusselt number and Sherwood number respectively as

$$C_f Re_x^{\frac{1}{2}} = f''(0),$$
$$Nu_x Re_x^{-\frac{1}{2}} = -\theta'(0),$$
$$Sh_x Re_x^{-\frac{1}{2}} = -\phi'(0). \quad (14)$$

Kuznetsov and Nield [5] referred $-\theta'(0)$ and $-\phi'(0)$ as the reduced Nusselt and Sherwood number, Nu_r and Sh_r respectively.

3 NUMERICAL METHODS

The coupled set of non-linear differential equations (7)-(9) along with the boundary conditions (10a) and (10b) form a three point BVP and does not form a closed form analytical solution. Therefore, it is solved numerically using fourth order classical 'Runge-Kutta Method'. In this method, we first convert the governing equations together with the boundary conditions into first order system.

$$y'_1 = y_2, y'_2 = y_3,$$
$$y'_3 = -[0.5 y_1 y_3 - \kappa_1(y_2 - 1) - \kappa_2(y_2^2 - 1)],$$
$$y'_4 = y_5, y'_5 = -P_r[N_b y_5 y_7 + N_t y_5^2 + 0.5 y_1 y_5], \text{and}$$
$$y'_6 = y_7, y'_6 = -\left[0.5 L_e y_1 y_7 + N_{tb} y'_5\right].$$

Where $y_1 = f, y_2 = f', y_3 = f'', y_4 = \theta, y_5 = \theta', y_6 = \phi, y_7 = \phi'$.

With the boundary conditions

$$f(0) = 0, f'(0) = 0, \theta(0) = 1 \text{ and } \phi(0) = 1.$$

The method employed is the Adaptive Runge-Kutta method (Dormand-prince method) which is implemented in MATLAB as an m-file in the form of ode. It automatically finds the appropriate step size $\Delta\eta$ by comparing the results of a fourth-order and fifth-order method. It requires size function evaluations per $\Delta\eta$, and construct a fourth-fifth order method from these function evaluations.

4. RESULTS AND DISCUSSION

A numerical computation as well as a parametric study is performed to illustrate the effect of several dimensionless parameters namely, the permeability parameter κ_1, the inertial parameter κ_2, the Prandtl number P_r, the Brownian motion parameter N_b, the thermophoresis parameter N_t, and the Lewis number Le. The effect of this parameters on the dimensionless flow properties such as velocity, shear stress, temperature, nanoparticle concentration, and the rate of heat and mass transfer are investigated numerically and presented graphically in Figs. (2-11). as a test of the accuracy of the method used, the values of $f''(0)$ for non-porous plate $\kappa_1 = \kappa_2 = 0$ are compared with the values reported by Blasius [18], Howarth [19], Cortell [20], Ishak et al. [15] and Bhattacharyya et al. [21] for wall skin friction in Table 1. This table shows that the numerical results obtained by the present method of solution are in very good agreement with the previous results. Table 2: shows the numerical values of reduced Nusselt number Nu and reduced Sherwood number S_h for various values of N_t and N_b. The results are compared

with those in literature reported by Khan and Pop [4], Makinde and Aziz [22], Md. Jashim Uddin et al. [23], Noghrehabadi et al. [24] and the comparison are found to be in good agreement for each value of N_t and N_b when $Le = P_r = 10$, $\kappa_1 = \kappa_2 = 0$. The choice of the values of κ_1 and κ_2 depends on the porosity of the regime and the kinetic energy of the fluid. Prandtl number of 0.71 is chosen for air while other values were chosen arbitrarily. Values of N_t and N_b were chosen base on the fact that these values were used by Khan and Pop [4] and Makinde and Aziz [22]. Fig. 1: (a)-(d) illustrates the velocity profiles for different values of the permeability of the medium and the inertial parameter effects respectively while the other parameters are kept constant. Fig. 1: (a) and (b) shows the effect of increasing values of porosity at low and high kinetic energy of the system. At low kinetic energy, it is observed that an increases in permeability of the medium causes the horizontal velocity of the flow to increase, therefore leading to a decrease in the thickness of the velocity boundary layer. The Darcian body force also decreases (i.e. flow retardation decreases) as it is inversely proportional to the permeability. As the inertia effect dominates the system of flow, the kinetic energy increases, the velocity also increases and the curves become steeper, and the effect of the permeability becomes less pronounce at this stage. From Fig. 1: (c) and (d) it is noted that an increase in the inertial parameter leads to an increase in the velocity profile with much wider distribution at low and higher permeability of the medium when compared with the first two cases. This actually shows the significant effect of the Forchheimer term on the velocity distribution. In all the velocity curves, the rate of transport increases with increasing boundary layer thickness η, and varnishes or approaches 0.9999 asymptotically at a distance of $\eta = 4$ for Fig. 1: (b) and 1(d) and $\eta = 5$ for Fig. 1: (a) and 1(c).

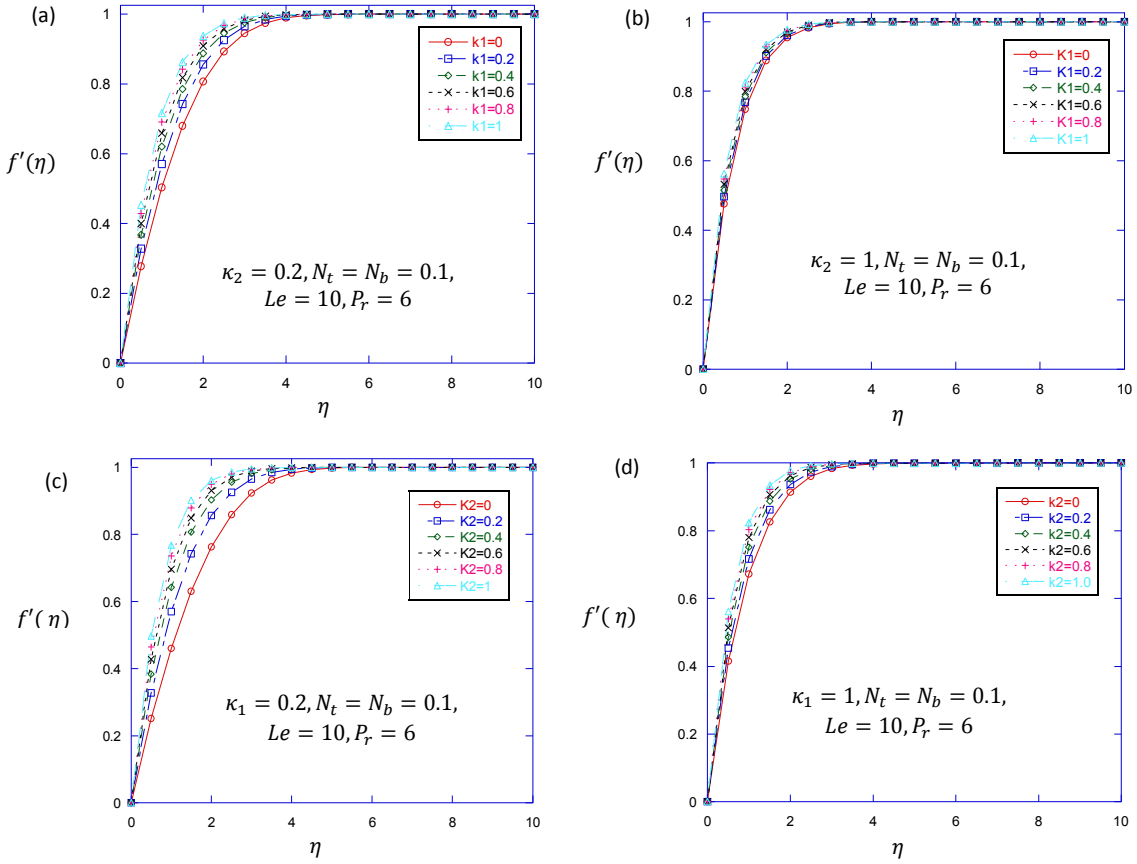

Fig. 1. (a)Velocity profile vs η when $\kappa_2 = 0.2$, (b) when $\kappa_2 = 1$, (c) when $\kappa_1 = 0.2$, (d) when $\kappa_1 = 1$

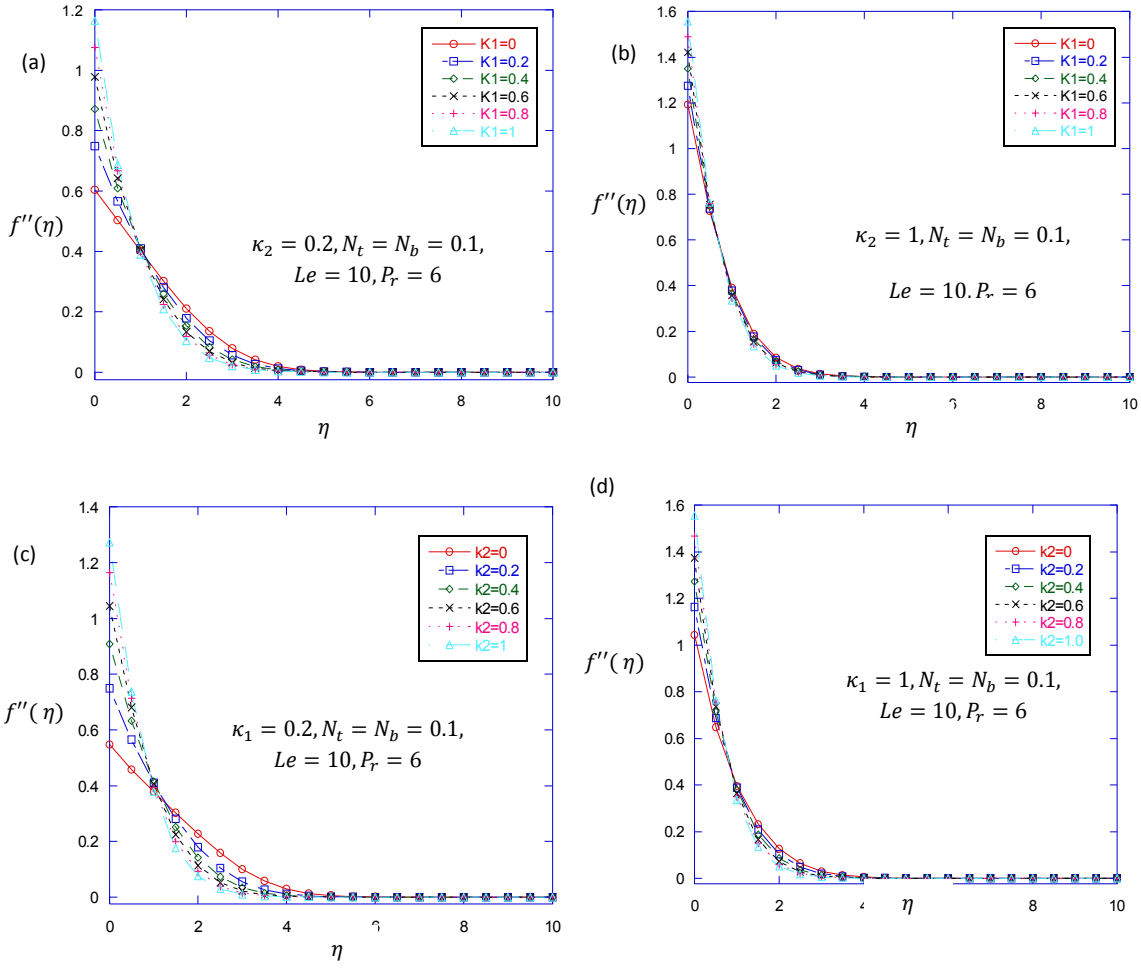

Fig. 2. (a) Shear stress vs when $\kappa_2 = 0.2$, (b) when $\kappa_2 = 1$, (c) when $\kappa_1 = 0.2$, (d) when $\kappa_1 = 1$

Table 1. Comparison of $f''(0)$ for non-porous plate

Blasius [18]	Howarth [19]	Cortell [20]	Ishak et al. [15]	Swati et al. [25]	Present study
0.332	0.33206	0.33206	0.3321	0.33206	0.3321

Fig. 2: (a)-(d) represents the shear stress profiles for different values of permeability and inertial parameter of the medium. Fig. 2: (a) and (b) depicts the effect of permeability parameter at low and high inertia of the system. In both cases, shear stress is found to have decrease, with the decreases been higher at much higher kinetic energy. Fig. 2: (c) and (d) exhibit the effect of the inertial parameter at low and high permeability. It is observed that the inertial parameter decreases the shear stress in both cases and the decrease has been more pronounce at higher permeability.

Fig. 3: (a)-(d) shows the effect of permeability parameter on temperature at low and high inertial parameter and the effect of the inertial parameter on temperature at low and high permeability of the medium. We notice that, both permeability and inertial parameter decrease temperature when either of the two is low. This effect can be use as a method of cooling. When both parameters are high, the decrease in temperature is very small. Fig. 4: (a) and (b) illustrate the effect of Thermophoresis and Brownian motion parameter on the temperature respectively. Both parameters increase

temperature. The effect of Thermophoresis, Brownian motion, permeability and inertia on the Nanoparticle concentration is shown in Fig. 5: (a)-(f). It is shown that thermophoretic effect on concentration increases at lower Brownian diffusion with disturbance, while as both parameters increases simultaneously, the Brownian motion tends to reduce the effect of the thermophoresis parameter and hence the system is less disturbed. From Fig 5(c) and 5(d), it is observed that as Brownian motion increases while thermophoresis is low, concentration decreases. As both parameters increase simultaneously, concentration decreases and the system is disturbed. Fig. 5(e) and 5(f) illustrate the effect of permeability and inertia on the concentration profile. It is depicted that both parameters decreases concentration, with inertia decreasing the concentration at a wider distribution.

Fig. 6: (a) and (b) shows the effect of P_r and Le number on the temperature profile respectively. An increase in Prandtl number leads to a decrease in temperature. Lewis number also decreases temperature, but its effect is very small. The effect of these parameters on concentration is shown in Fig. 7: (a) and (b). It is observed that concentration increases as the Prandtl number increases, but decreases with increase in Lewis number. This is as a result of the decrease in nanoparticle boundary layer thickness when the Lewis number increases. Fig. 8: (a)-(c) illustrate the effect of permeability on the skin friction, heat and mass transfer respectively. With increase in permeability, skin friction increases as well as heat and mass transfer with increasing inertial parameter. Fig. 9: (a)-(c) shows the effect of the inertial parameter on the skin friction, heat and mass transfer respectively. As the inertial parameter increases,

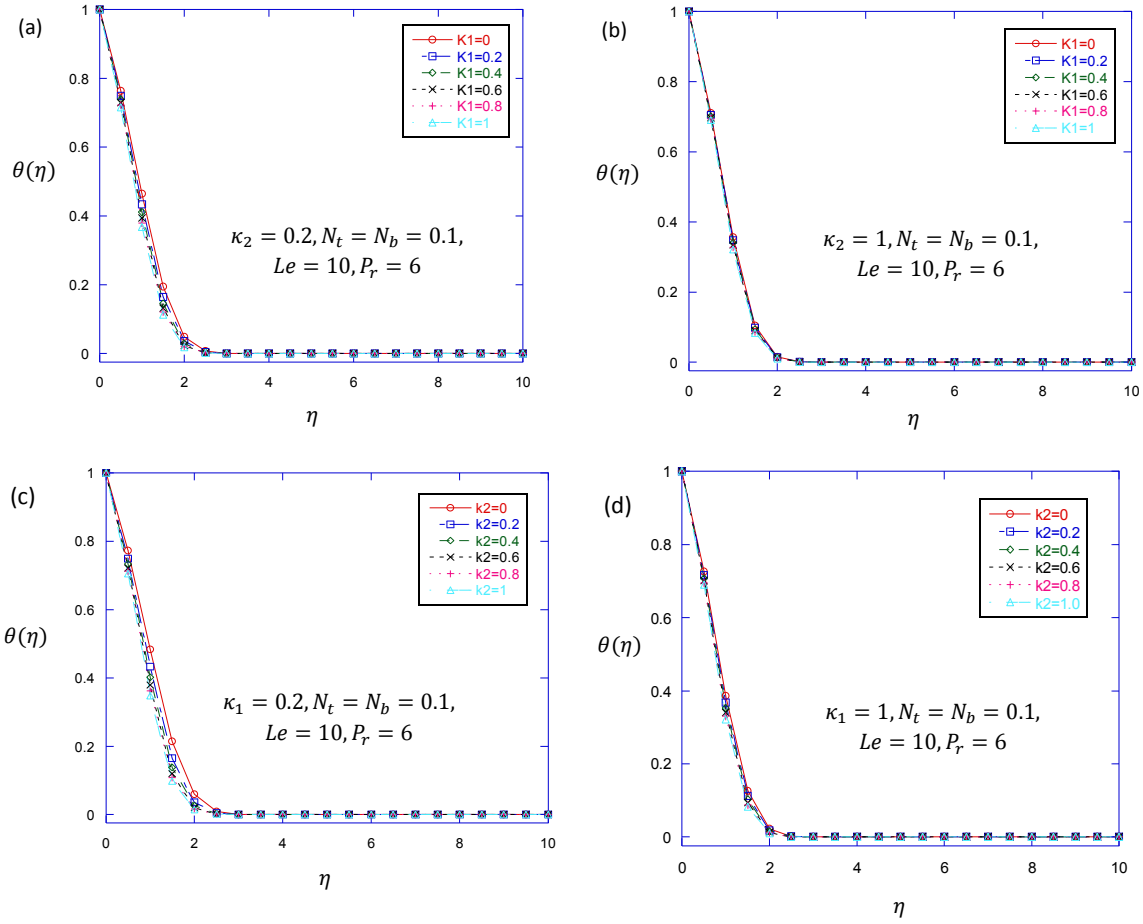

Fig. 3. (a)Temperature distribution vs η when $\kappa_2 = 0.2$, (b)when $\kappa_2 = 1$, (c)when $\kappa_1 = 0.2$, (d) when $\kappa_1 = 1$

the skin friction, heat and mass transfer increases. The influence of thermophoresis on heat and mass transfer with increasing Brownian motion is shown in Fig. 10: (a) and (b). It is shown that heat transfer decreases with increasing thermophoresis while mass transfer increases as the thermophoretic number increase. Fig: 11: (a) and (b) shows Brownian motion effect on the heat and mass transfer. It has been noticed that both heat and mass transfer decreases with increase in Brownian motion parameter. Table 3: shows the numerical values of $-\theta'(0)$ and $-\phi'(0)$ for various values of N_t when $Le = 10$ and $P_r = 6.0$. It can be seen that the reduced Nusselt number is a decreasing function, while the reduced sherwood number is an increasing function of the thermophoretic number N_t.

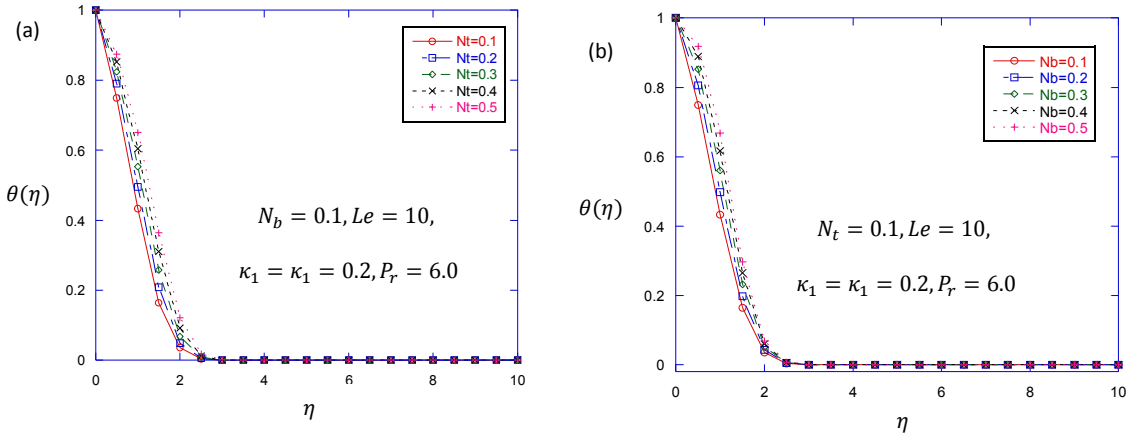

Fig. 4. (a) Temperature distribution vs η *when* $N_b = 0.1$, (b) *when* $N_t = 0.1$

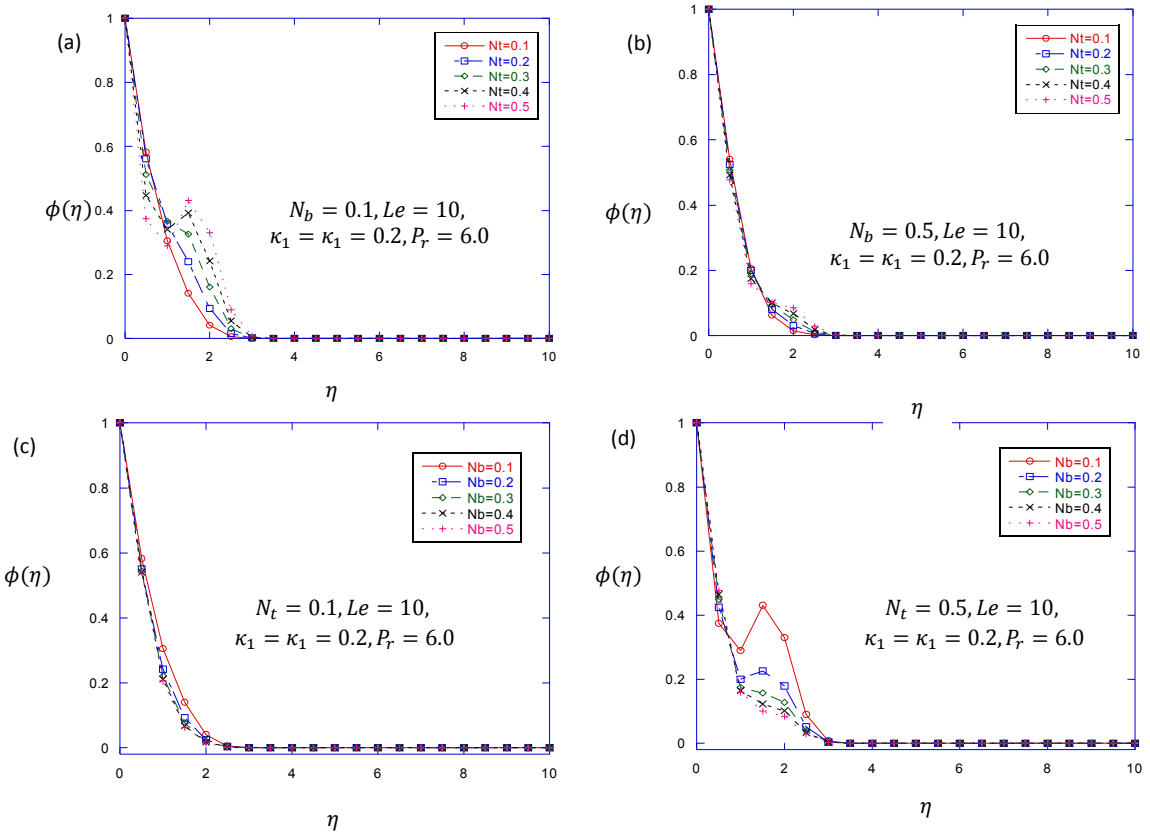

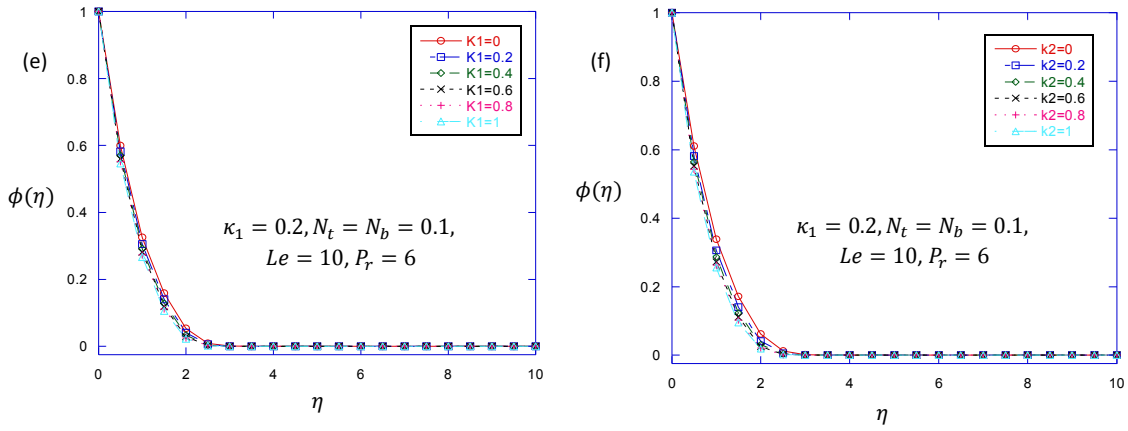

Fig. 5. (a)Concentration distribution vs η when$N_b = 0.1$ (b) when $N_b = 0.5$ (c) when $N_t = 0.1$(d) when $N_t = 0.5$ (e) when $\kappa_2 = 0.2$ (f) when $\kappa_1 = 0.2$

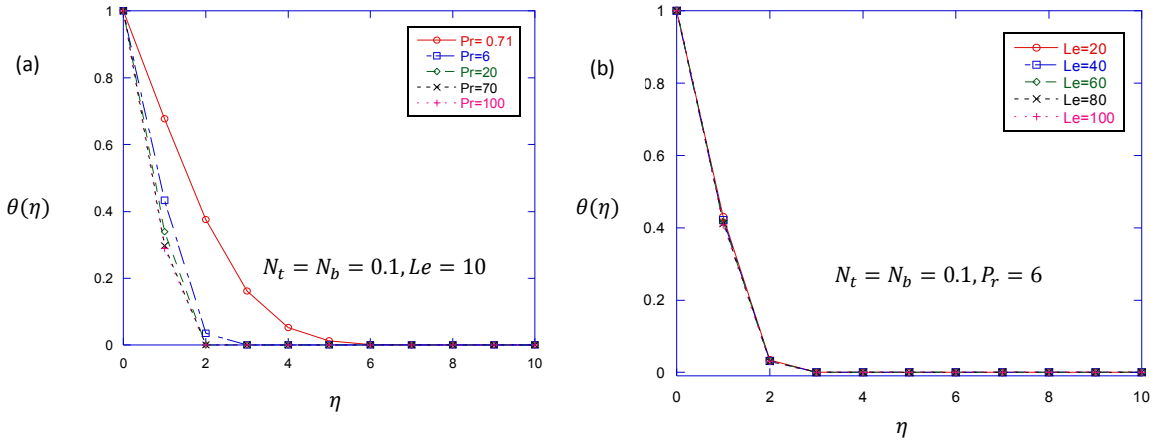

Fig. 6. (a) Temperature distribution vs η for different values of P_r (b) for different values of Le

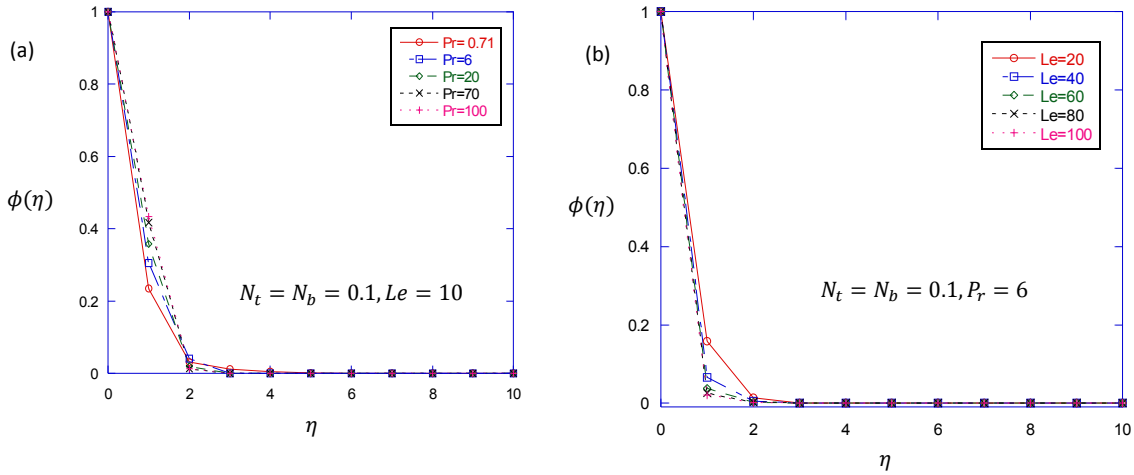

Fig. 7. (a)Concentration distribution vs η for different values of P_r (b) for different values of Le

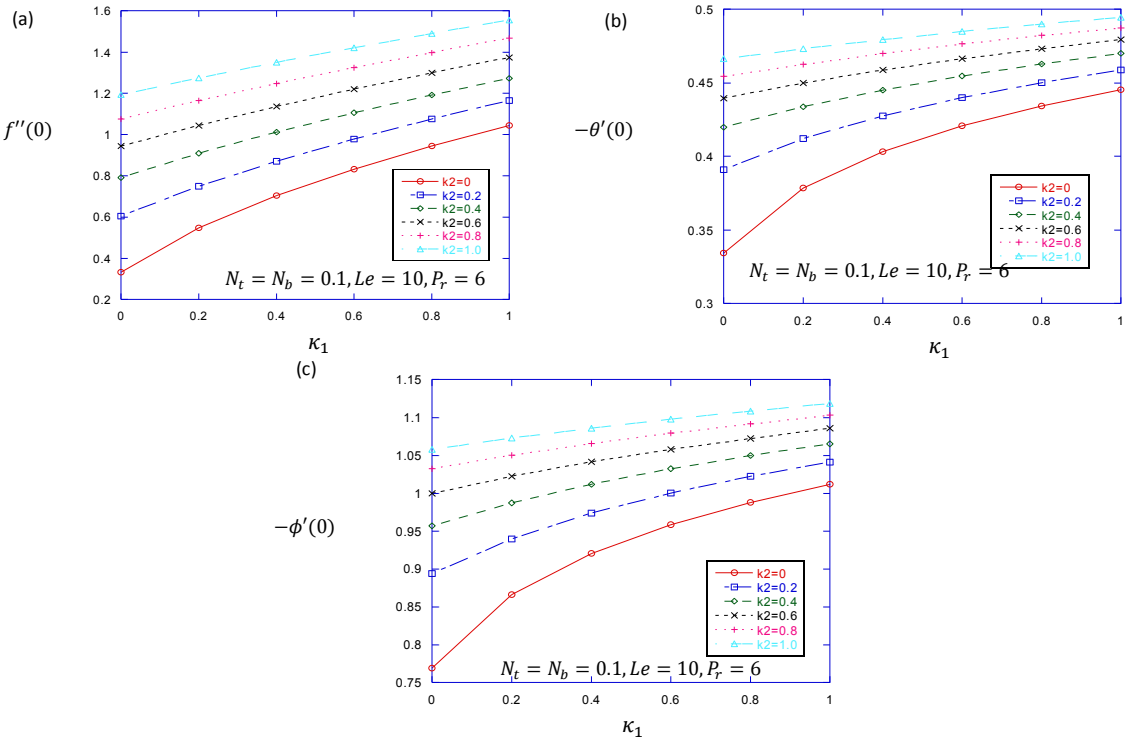

Fig. 8. (a)Skin friction vs κ_1 (b) Heat transfer vs κ_1 (c) Mass transfer vs κ_1

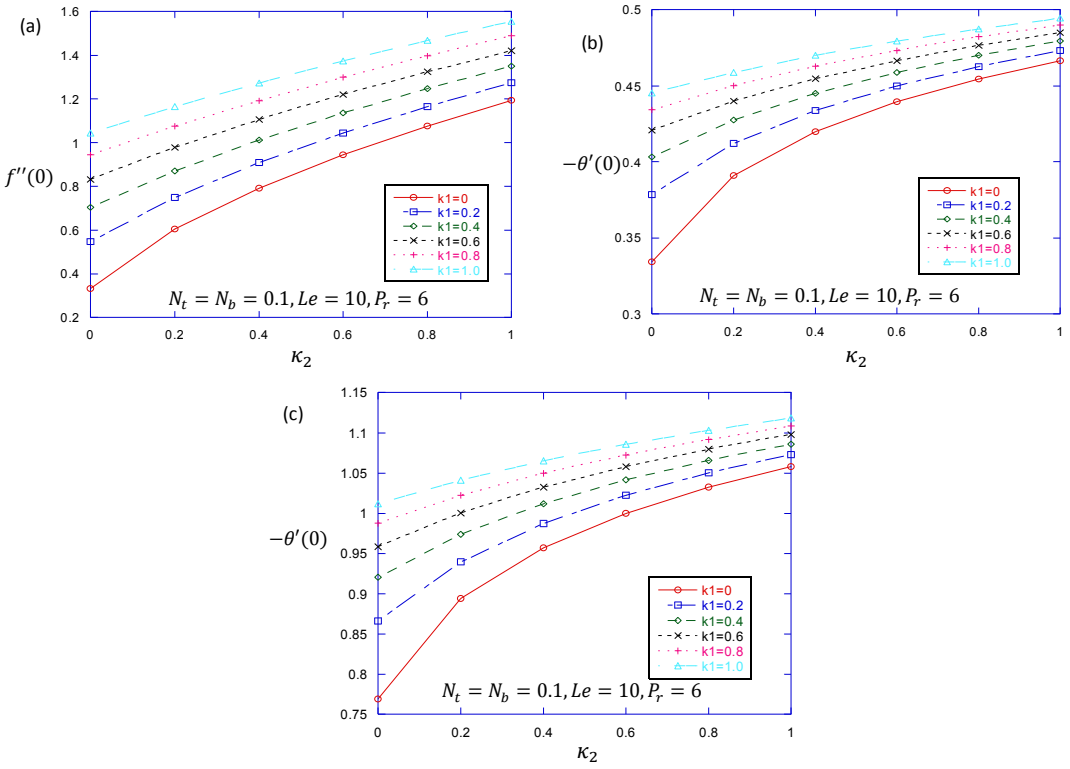

Fig. 9. (a)Skin friction vs κ_2 (a) Heat transfer vs κ_2 (c) Mass transfer vs κ_2

Table 2. Comparison of results for reduced Nusselt number $-\theta'(0)$ and reduced Sherwood number $-\phi'(0)$ with $Le = P_r = 10, \kappa_1 = \kappa_2 = 0$

N_b	N_t	Khan and Pop [4]		Makinde and Aziz [22]		Md. Jashim Uddin et al. [23]		Noghrehabadi et al. [24]		Present result	
		$-\theta'(0)$	$-\phi'(0)$	$-\theta'(0)$	$-\phi'(0)$	$-\theta'(0)$	$-\phi'(0)$	$-\theta'(0)$	$-\phi'(0)$	$-\theta'(0)$	$-\phi'(0)$
0.1	0.1	0.9524	2.1294	0.9524	2.1294	0.95238	2.12939	0.95238	-	0.9524	2.1294
0.2	0.1	0.5056	2.3819	0.5056	2.3819	0.50558	2.38187	0.50558	-	0.5056	2.3819
0.3	0.1	0.2522	2.4100	0.2522	2.4100	0.25216	2.41002	0.25216	-	0.2522	2.4100
0.4	0.1	0.1194	2.3997	0.1194	2.3997	0.11946	2.39965	-	-	0.1194	2.3997
0.5	0.1	0.0543	2.3836	0.0543	2.3836	0.05425	2.38357	-	-	0.0543	2.3836
0.1	0.2	0.6932	2.2740	0.6932	2.2740	0.69317	2.27401	0.69317	-	0.6932	2.2740
0.1	0.3	0.5201	2.5286	0.5201	2.5286	0.52008	2.52863	0.52008	-	0.5201	2.5286
0.1	0.4	0.4026	2.7952	0.4026	2.7952	0.40258	2.79515	-	-	0.4026	2.7952
0.1	0.5	0.3211	3.03512	0.3211	3.03512	0.32105	3.03512	-	-	0.3211	3.03512

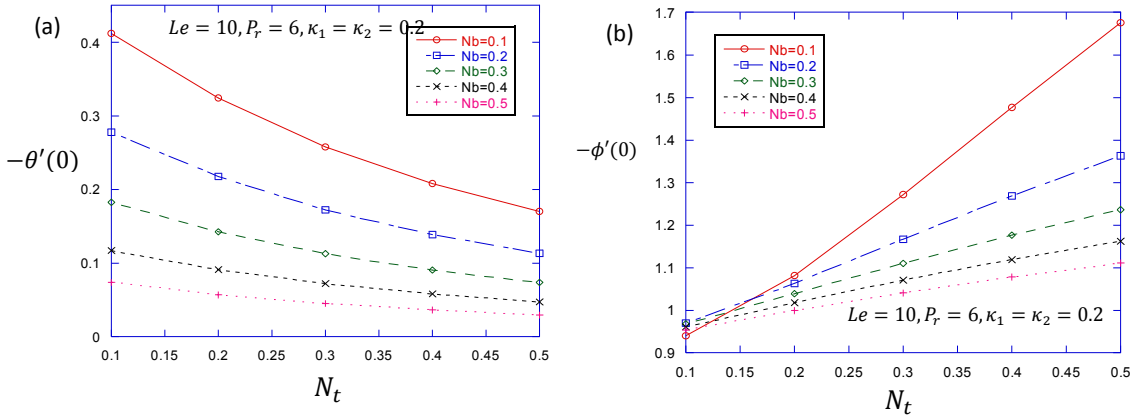

Fig. 10. (a)Heat transfer vs N_t (b) Mass transfer vs N_t

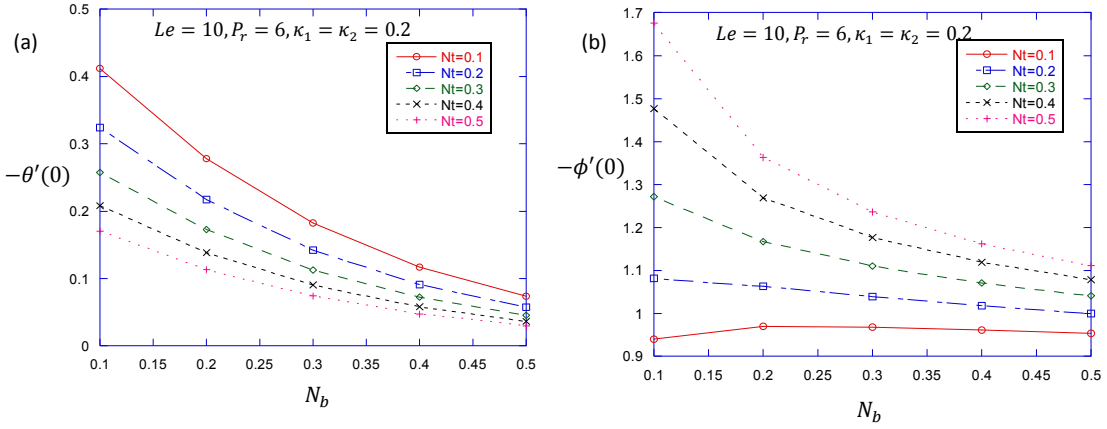

Fig. 11. (a)Heat transfer vs N_b (b) Mass transfer vs N_b

Table 3. Numerical values of $-\theta'(0)$ and $-\phi'(0)$ for different values of N_t when $\kappa_1 = \kappa_2 = 0.2, Le = 10$ and $P_r = 6$

N_b	N_t	$-\theta'(0)$	$-\phi'(0)$
0.1	0.1	0.41209	0.93995
	0.2	0.32401	1.0815
	0.3	0.25791	1.27214
	0.4	0.20813	1.47679
	0.5	0.17041	1.67587
0.2	0.1	0.27801	0.96981
	0.2	0.21750	1.06339
	0.3	0.17255	1.16654
	0.4	0.13895	1.2683
	0.5	0.11361	1.3630
0.3	0.1	0.18268	0.96829
	0.2	0.14244	1.03931
	0.3	0.11276	1.1101
	0.4	0.09068	1.17644
	0.5	0.07408	1.23643

5. CONCLUSIONS

This study has analyzed the flow, heat and mass transfer of a nanofluid over a porous plate in a Darcy-Forchheimer flow numerically. By using the similarity transformation approach, the governing partial differential equations are transformed into non-linear ordinary differential equations and the resulting problem is solved using Runge-Kutta method. The influence of the governing parameters on the flow, heat and mass transfer has been closely examined. The following conclusions are drawn from the analysis:

1. The velocity of the flow accelerates with an increase in the inertial and permeability of the medium
2. The temperature of the flow rises with an increase in the thermophoretic number , the Brownian motion parameter and fall with an increase in the permeability of the medium, the inertial parameter, the Prandtl number and the Lewis number
3. Nanoparticle concentration increases with an increasing thermophoresis and Prandtl number and decreases with an increase in permeability, inertia, Brownian motion and Lewis number
4. Skin friction coefficient increases with an increase in permeability and the inertia parameter of the medium
5. Heat transfer rate rises with an increase in permeability, the inertia and Prandtl number (for fluids with P_r number between 0.71 and 6, and decreases for fluids with higher Prandtl numbers). The rate falls with an increase in Brownian motion, thermophoresis and Lewis number
6. Mass transfer rate increases with an increase in permeability, inertia, thermophoresis, Prandtl number and Lewis number and decreases with an increase in Brownian motion

COMPETING INTERESTS

Authors have declared that no competing interests exist.

REFERENCES

1. Choi S. American Society of Mechanical Engineers. 1995;99-105.
2. Buongiorno J. Convective transport in nanofluids. ASME Journal of Heat Transfer. 2006;128:240-250.

3. Ellani R, Hassan M, Zeeshan A. Shape effects of nanosize particles in Cu-H_20 nanofluid on entropy generation. International Journal of Heat and Mass Transfer. 2015;81:449-456.
4. Khan WA, Pop I. Boundary layer flow of nanofluid over a stretching sheet. International Journal of Heat and Mass Transfer. 2010;53(11-12):2477-2483.
5. Kuznetsov VA, Nield DA. Effect of nanoparticles on the natural convection boundary layer flow past a vertical plate. International Journal of Thermal Sciences. 2010;49(2):243-247.
6. Rahman SU, Ellahi R, Sohail Nadeem, Zaigham Zia QM. Simultaneous effects of nanoparticles and slip on Jeffrey fluid through tapered artery with mild stenosis. Journal of Molecular Liquids. 2016;218: 484-493.
7. Zeeshan A, Majeed, Ellahi. Effect of magnetic dipole on viscous ferro-fluid past a stretching surface with thermal radiation. Journal of Molecular Liquids. 2016;215: 549-554.
8. Mohsen Sheikholeslami, Rahmat Ellani. Electrohydrodynamic nanofluid hydro-thermal treatment in an enclosure with sinusoidal upper wall. Applied Science. 2015;5:294-306.
9. Sheikholeslami Mohsen, Domiri Ganji Davood, Younus Javed M, Ellahi R. Effect of thermal radiation on nanofluid flow and heat transfer using two phase model. Journal of Magnetism and Magnetic Materials. 2015;374:36-43.
10. Ellahi Rahman, Hassan Mohsin, Zeeshan Ahmad. Study of natural convection MHD nanofluid by means of single and multi-walled carbon nanotubes suspended in a salt water solution. IEEE Transactions in Nanotechnology. 2015;14(4):726-734.
11. Kandelousi Mohsen Sheikholeslami, Ellahi Rahamat. Simulation of ferrofluid flow for magnetic drug targeting using lattice boltzmann method. Journal of Zeitschrift Fur Naturforschung A, Verlag Der Zeitschrift Für Naturforschung. 2015;70(2): 115-124.
12. Saman Rashidi, Maziar Dehghan, Ellahi R, Milad Tajik Jamal-Abad. Study of stream wise transverse magnetic fluid flow with heat transfer around a porous obstacle. Journal of Magnetism and Magnetic Materials. 2015;378:128-137.
13. Sher Akbar Noreen, Raza M, Ellahi R. Influence of induced magnetic field and heat flux with the suspension of carbon nanotubes for the peristaltic flow in a permeable channel. Journal of Magnetism and Magnetic Materials. 2015;381:405-415.
14. Sheikholeslami M, Ellahi R. Three dimensional mesoscopic simulation of magnetic field effect on natural convection of nanofluid. International Journal of Heat and Mass Transfer. 2015;89:799-808.
15. Ishak A, Nazar R, Pop I. Steady and unsteady boundary layers due to a stretching vertical sheet in a porous medium using Darcy-Brinkman equation model. International Journal of Applied Mechanical Engineering. 2006;11(3):623-637.
16. Bear J. Dynamics of fluids in porous media. Dover, New York; 1972.
17. Chen CK, Chen CH, Minkowycz, Gill US. Non-Darcian effects on mixed convection about a vertical cylinder embedded in a saturated porous. International Journal of Heat and Mass Transfer. 1992;35:3041-3046.
18. Blasius H. Grenzschichten in flussigkeiten mit kleiner reibung. Zeitschrift fur Mathematik und Physik. 1908;56:1-37.
19. Howarth L. On the solution of the laminar boundary layer equations. Proceedings of the Royal Society London. 1938;164:547-579.
20. Cortell R. A numerical tackling on Sakiadis flow with thermal radiation. Chin. Phys. Lett. 2008;25:1340-1342.
21. Bhattacharyya K, Swati M, Layek GC. Steady boundary layer slip flow and heat transfer over a flat porous plate embedded in a porous media. Journal of Petroleum Science and Engineering. 2011;78:304-309.
22. Makinde OD, Aziz A. Boundary layer flow of a nanofluid past a stretching sheet with a convective boundary condition. International Journal of Thermal Sciences. 2011;50:1326-1332.
23. Md. Jashim Uddin, Khan WA, Md. Ismail AI. Scaling group transformation for MHD boundary layer slip flow of a nanofluid over a convectively heated stretching sheet with heat generation. Mathematical Problems in Engineering. 2012;20.
24. Aminreza Noghrehabadi, Mohammed Reza S, Rashid Pourrajab, Mohammad

Ghalambaz. Entropy analysis for nanofluid flow over a stretching sheet in the presence of heat generation/absorption and partial slip. Journal of Mechanical Science and Technology. 2013;27:927-937.

25. Swati M, Prativa Ranjan De, Bhattacharyya K, Layek GC. Forced convective flow and heat transfer over a porous plate in a Darcy Forchheimer porous medium in presence of radiation. Meccanica. 2012;47:153-161.

Peer-review history:
The peer review history for this paper can be accessed here:
http://www.sdiarticle3.com/review-history/26905